

# Characterization of Fluorescent Proteins with Intramolecular Photostabilization\*\*

Sarah S. Henrikus,<sup>[a, b, f]</sup> Konstantinos Tassis,<sup>[a]</sup> Lei Zhang,<sup>[c]</sup> Jasper H. M. van der Velde,<sup>[a]</sup> Christian Gebhardt,<sup>[c]</sup> Andreas Herrmann,<sup>[d, e]</sup> Gregor Jung,<sup>[b]</sup> and Thorben Cordes\*<sup>[a, c]</sup>

Genetically encodable fluorescent proteins have revolutionized biological imaging *in vivo* and *in vitro*. Despite their importance, their photophysical properties, i.e., brightness, count-rate and photostability, are relatively poor compared to synthetic organic fluorophores or quantum dots. Intramolecular photostabilizers were recently rediscovered as an effective approach to improve photophysical properties of organic fluorophores. Here, direct conjugation of triplet-state quenchers or redox-active substances creates high local concentrations of photostabilizer around the fluorophore. In this paper, we screen for effects of covalently linked photostabilizers on fluorescent proteins. We produced a double cysteine mutant (A206C/L221C) of  $\alpha$ -GFP for attachment of photostabilizer-maleimides

on the  $\beta$ -barrel near the chromophore. Whereas labelling with photostabilizers such as trolox, a nitrophenyl group, and cyclo-octatetraene, which are often used for organic fluorophores, had no effect on  $\alpha$ -GFP-photostability, a substantial increase of photostability was found upon conjugation to azobenzene. Although the mechanism of the photostabilizing effects remains to be elucidated, we speculate that the higher triplet-energy of azobenzene might be crucial for triplet-quenching of fluorophores in the blue spectral range. Our study paves the way for the development of fluorescent proteins with photostabilizers in the protein barrel by methods such as unnatural amino acid incorporation.

## 1. Introduction

Fluorescent proteins (FPs) have revolutionized fluorescence imaging of biological systems *in vivo* and *in vitro*. Because they are genetically encoded, they allow the tethering of a natural light-emitting protein chromophore to any protein of interest.<sup>[1–3]</sup> Since there are no other fluorescent tags with these properties, the impact of FPs for biological research cannot be overemphasized.<sup>[1,3–5]</sup> Despite their importance, the photophysical properties of FPs, i.e., brightness, count-rate and photostability,<sup>[6–8]</sup> are relatively poor compared to synthetic organic fluorophores<sup>[9]</sup> or quantum dots.<sup>[10,11]</sup> For example the brightness of the fluorescent dye Cy3B is three times higher than for eGFP.<sup>[12]</sup> Extensive research has been done over the past decades to improve the photophysical properties of FPs.<sup>[13]</sup> These studies have resulted in numerous FP-variants<sup>[14–16]</sup> with

useful chemical and photophysical properties, such as variants optimized for fast folding,<sup>[17,18]</sup> photoswitching,<sup>[19]</sup> and brightness,<sup>[8,20,21]</sup> or for functions such as pH sensing.<sup>[22]</sup> Yet, there are no FPs with photophysical properties that can compete with synthetic dyes in terms of brightness and photostability.<sup>[6]</sup>

Intramolecular triplet-state quenchers were recently rediscovered as an attractive approach for photostabilization in various fluorescence applications.<sup>[23,24]</sup> The approach was already proposed and experimentally realized in the 1980s<sup>[25,26]</sup> and uses direct conjugation of photostabilizing compounds such as triplet-state quenchers or redox-active substances to a fluorescent reporter (typically a synthetic organic fluorophore), thereby creating high local concentrations of photostabilizer around the fluorophore.<sup>[27]</sup> As illustrated in Figure 1, this improves the photophysical properties of organic dyes such as Cy5 in bulk

[a] Dr. S. S. Henrikus, K. Tassis, Dr. J. H. M. van der Velde, Prof. Dr. T. Cordes  
Molecular Microscopy Research Group,  
Zernike Institute for Advanced Materials,  
University of Groningen  
Nijenborgh 4, 9747 AG Groningen (The Netherlands)

[b] Dr. S. S. Henrikus, Prof. G. Jung  
Biophysical Chemistry,  
Saarland University  
Campus Building B2.2, 66123 Saarbrücken (Germany)

[c] Dr. L. Zhang, C. Gebhardt, Prof. Dr. T. Cordes  
Faculty of Biology, Physical and Synthetic Biology,  
Ludwig-Maximilians-Universität München  
Großhadernerstr. 2–4, 82152 München – Planegg-Martinsried (Germany)  
E-mail: cordes@bio.lmu.de


[d] Prof. A. Herrmann  
Department of Polymer Chemistry,  
Zernike Institute for Advanced Materials,  
University of Groningen  
Nijenborgh 4, 9747 AG Groningen (The Netherlands)

[e] Prof. A. Herrmann  
DWI – Leibniz Institute for Interactive Materials  
Forckenbeckstr. 50, 52056 Aachen (Germany)

[f] Dr. S. S. Henrikus  
Current address: Francis Crick Institute  
1 Midland Road, London NW1 AT1 (UK)

[\*\*] A previous version of this manuscript has been deposited on a preprint server (<https://doi.org/10.1101/2020.03.07.980722>).

 Supporting information for this article is available on the WWW under <https://doi.org/10.1002/cbic.202100276>

 © 2021 The Authors. ChemBioChem published by Wiley-VCH GmbH. This is an open access article under the terms of the Creative Commons Attribution Non-Commercial License, which permits use, distribution and reproduction in any medium, provided the original work is properly cited and is not used for commercial purposes.

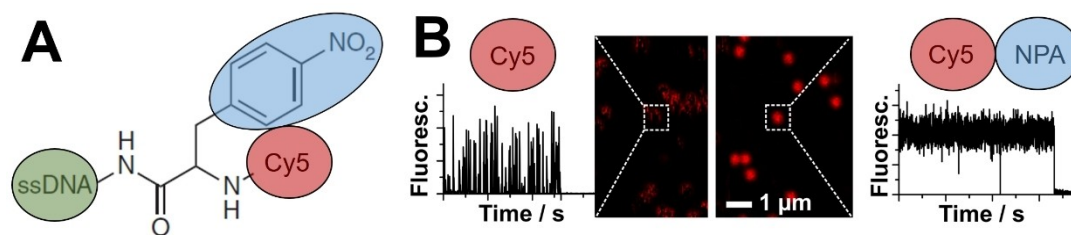


**Figure 1.** (A) Structure of a self-healing organic NPA-Cy5 fluorophore on an oligonucleotide structure. (B) Experimental demonstration of photostability increases of Cy5 that are simultaneously coupled to a biomolecule (left) and to a photostabilizer (right). Analysis of single-molecule fluorescence microscopy data shows temporal behavior of fluorescence emission of ‘self-healing’ fluorophore and confocal scanning images and time traces from self-healing Cy5 fluorophores on oligonucleotides. Data were reprinted from Ref. [27].

and single-molecule investigations *via* intramolecular quenching of triplet or radical states (mediated in the concrete example by the nitrophenylalanine (NPA) group; data from Ref. [27]).

Such a strategy obviates the need for complex buffer systems, and makes these dyes with intramolecular photostabilization “self-healing”, and thus compatible with diverse biological systems.<sup>[23,24,27–30]</sup> This is a particular advantage in situations in which the fluorescent dye is inaccessible to exogenously added stabilizers (e.g., when contained in certain biological cell-compartments<sup>[31]</sup>). Based on new mechanistic insights,<sup>[32,33]</sup> there has been exciting progress on the optimization of the photostabilization efficiencies in self-healing dyes,<sup>[31,34–36]</sup> the development of bioconjugation strategies for different fluorophore types,<sup>[27]</sup> photostabilizers and biomolecules,<sup>[27,37]</sup> and their applications in super-resolution,<sup>[23,27,38]</sup> live-cell and single-molecule imaging. All this activity, however, has so far been focused on the major classes of synthetic organic fluorophores including rhodamines,<sup>[24,27,34,38]</sup> cyanines,<sup>[23,27,29,31,35,36]</sup> carbopyronines,<sup>[38]</sup> bophy-dyes,<sup>[39]</sup> oxazines<sup>[37]</sup> and fluoresceins.<sup>[37]</sup> The recent direct and unambiguous demonstration of the formation of a long-lived chromophore triplet state in green fluorescent proteins<sup>[40]</sup> suggests that intramolecular photostabilization may be a strategy applicable to fluorescent proteins as well.

The green fluorescent protein (GFP) was discovered by Shimomura et al. in the jellyfish *Aequorea victoria* (avGFP) in 1962.<sup>[5]</sup> The 27 kDa protein shows a secondary structure made up of eleven  $\beta$ -strands, two short  $\alpha$ -helices and the chromophore in the center. The  $\beta$ -strands form an almost perfect barrel, which is capped at both ends by  $\alpha$ -helices.<sup>[41]</sup> Therefore the para-hydroxybenzylidene-imidazolinone chromophore in the center of the  $\beta$ -barrel is separated from exterior.<sup>[42]</sup> The dimension of the cylinder are about 4.2 by 2.4 nm. Proper folding is required for autocatalytic maturation of the chromophore from the amino acids Ser65, Tyr66 and Gly67.<sup>[42]</sup> GFP shows green fluorescence after excitation in the near UV and blue spectral region. A major and minor absorption peak at 395 nm and 475 nm, respectively, describes the spectral characteristics of GFP. Fluorescence emission occurs either at 503 nm (excitation at 475 nm) or 508 nm (excitation at 395 nm). The two emission peaks belong to the anionic form of GFP;

excellent summaries of GFP photophysics are provided in Refs. [16,43,44].

Here, we introduce an experimental strategy to screen for the effects of covalently linked photostabilizers on the photophysical behavior of fluorescent proteins. For this, we recombinantly produced a double cysteine mutant (A206C/L221C, Figure S1) of alpha-GFP (F99S/M153T/V163A)<sup>[45]</sup> for attachment of photostabilizer-maleimide conjugates. The cysteines did not influence the fluorescence parameters, i.e., spectrum and quantum yield, of the protein and also labelling with cyclo-octatetraene (COT), trolox (TX) and a nitrophenyl-group showed negligible effects. Strikingly, we found a substantial increase of photostability upon conjugation to the azobenzene (AB) derivative, 4-phenylazomaleinanyl (4-PAM, Figure S1C). Although the mechanism underlying FP-photostabilization by azobenzene remains to be elucidated, our study paves the way towards the development and design of a second generation of fluorescent proteins with photostabilizers placed directly in the protein barrel by methods such as unnatural amino acid incorporation.

## 2. Results

A key obstacle in designing our research was the complex photophysical behavior of FPs, which meant that not only the properties of the chromophore itself, but also factors such as the  $\beta$ -barrel structure/biochemical state and the specific environment of the proteins had to be considered.<sup>[46–49]</sup> Although unnatural amino acid incorporation does present an attractive strategy for the introduction of a photostabilizer into an FP, this route seemed challenging due to low protein expression levels or incorrect protein folding. Therefore, we decided for a strategy where photostabilizers can be covalently linked to GFP *via* thiomaleimide chemistry (Figure 2A).

For this, we produced a double cysteine mutant of  $\alpha$ -GFP, a GFP variant with mutations F99S/M153T/V163A as compared to wildtype GFP. We call this variant GFP-QC2 since it additionally contains two solvent-accessible cysteine residues (A206C, L221C, Figure 2A). The side chains of A206 and L221 are directed to the outside of the  $\beta$ -barrel, and therefore, following cysteine substitution of these residues, and labelling, photostabilizers can be placed outside of the barrel.

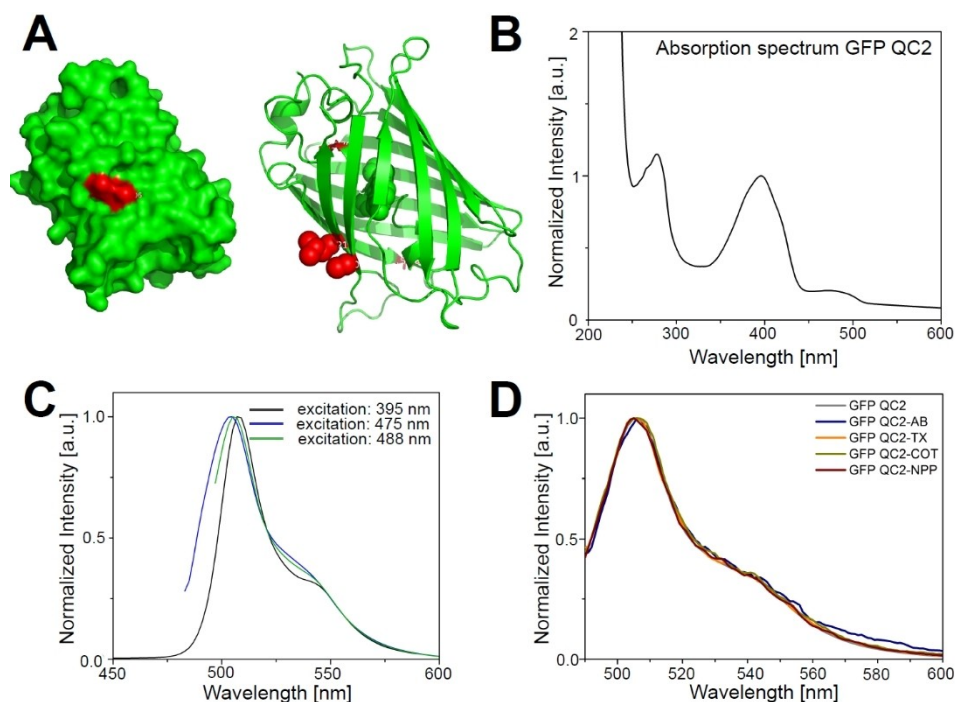


**Figure 2.** (A) Crystal structure of GFP-QC2 indicating residues A206 and L221 in red. These residues were substituted by cysteines in this study for attachment of maleimide photostabilizers. (B) Absorbance and (C) emission spectra, and (D) normalized emission spectra of unlabeled and labeled GFP-QC2.

The idea was that A206C and L221C (Figure 2A) would be points of attachment for photostabilizers that can affect the chromophore *via* changes of the protein-barrel<sup>[50]</sup> or alternatively *via* triplet energy-transfer processes using long-lived triplet-states.<sup>[40]</sup> While the latter are believed to occur more likely *via* Dexter-processes,<sup>[23,24]</sup> which would require collisions between FP chromophore and photostabilizer, there is support that certain triplet quenchers might utilize a Förster mechanism.<sup>[51]</sup> We thus reasoned that intramolecular triplet-quenching in FPs might not strictly require direct contacts between chromophore and stabilizer but proximity. This idea is strongly supported by the observation that FPs can also be influenced by solution-based photostabilizers (Figure S2 and Refs. [52–54]). Tinnefeld and co-workers<sup>[55]</sup> also demonstrated that EYFP shows a 6-fold enhanced photostability when using dSTORM/ROXS-buffer, i.e., a reducing-oxidizing buffer cocktail, oxygen removal and thiol addition, which should remain ineffective if the GFP-chromophore was fully inaccessible.

$\alpha$ -GFP contains two natural cysteines (C48, C70) which may have potentially interfered with our desired labeling of the barrel using maleimide chemistry. C48 is solvent-accessible, but too far away from the chromophore itself to be useful for photostabilizer attachment and was therefore removed by substitution for a serine residue (Figure S1A). In contrast, C70 is not solvent-accessible in the folded form of GFP, and was therefore not expected to interfere with labeling (Figure S1B). The final construct GFP-QC2 was verified by sequencing to carry the following mutations: C48S/F99S/M153T/V163A/A206C/L221C (Material and Methods and Figure S4).

The absorption and emission properties of GFP-QC2 were analyzed by steady-state spectroscopy methods,<sup>[27]</sup> and the results of these analysis are given in Figure 2/S3. The spectral characteristics of GFP-QC2 resembled those of  $\alpha$ -GFP.<sup>[56]</sup> The absorption spectrum of GFP-QC2 shows a main peak at  $\sim$ 395 nm (neutral chromophore) and a smaller peak at  $\sim$ 475 nm (anionic chromophore). In the UV range, absorbance by the aromatic amino acids tryptophan, tyrosine and phenylalanine dominate the absorption spectrum giving rise to an additional peak at  $\sim$ 280 nm. An important characteristic of the absorption spectrum was that the ratio of extinction coefficients of GFP-QC2 was slightly below  $\sim$ 1 at 280/395 nm.

Importantly, GFP-QC2 shows a fluorescence spectrum and quantum yield<sup>[56]</sup> of  $0.81 \pm 0.02$  (Figure S3) which resemble those of  $\alpha$ -GFP. Also the presence or absence of TCEP does not influence the spectra and quantum yield ( $0.81 \pm 0.01$ ), suggesting that cysteine oxidation or di-sulfide bridge formation does not occur in GFP-QC2. We also determined the quantum yield of eGFP to validate our method and found values of  $0.63 \pm 0.02$  and  $0.63 \pm 0.02$  in the absence and presence of TCEP, respectively (Figure S3). All this supports the idea that the cysteines A206 C/L221 C will provide anchor points for covalent attachment of photostabilizers, but do not influence the photophysics of the FP-chromophore, e.g., by modification of the  $\beta$ -barrel structure.

To test for intramolecular photostabilization, we compared the photophysical properties of unlabeled GFP-QC2 with labelled variants carrying the photostabilizers 4-PAM, Trolox (TX), cyclooctatetraene (COT) and nitrophenyl (NPP); see SI for details of photostabilizer synthesis. TX, COT and NPP are

photostabilizers that have been extensively used in self-healing dyes due to their triplet-state energy matching with organic fluorophores for Dexter-transfer (COT) or photo-induced electron-transfer (TX, NPP).<sup>[23,24,27–30]</sup> Azobenzene and stilbene, used in the original articles by Lüttke and co-workers for POPOP-dyes, are both known as potent quenchers of triplet-states.<sup>[57]</sup> Since solution-quenching of triplet-states with rate constants up to  $\sim 10^{10} \text{ M}^{-1} \text{ s}^{-1}$  were observed using azobenzene,<sup>[57]</sup> this molecule is generally an interesting candidate for both intra- and intermolecular photostabilization. Reasons for not selecting azobenzene earlier on in the development of self-healing dyes may have been caused by its additional ability to induce phototriggered conformational changes (in biological structural such as proteins<sup>[58–60]</sup>), which would require additional control of preserved biochemical function.

Labelling of GFP-QC2 was achieved using a protocol adapted from single-molecule Förster resonance energy transfer experiments (details see SI: 2. Material and Methods).<sup>[61]</sup> The labelling of GFP-azobenzene (GFP-AB) was monitored by size exclusion chromatography (Figure 3) *via* absorbance measurements at 280 nm (Trp/Tyr absorbance of GFP), 320 nm (4-PAM) and 395 nm (GFP chromophore). For GFP-QC2, the 280/395 ratio was just below 1 (Figure 3A), whereas it was just above 1 for GFP-AB (Figure 3B). These findings are consistent with the absorption spectrum of GFP-QC2 in Figure 2. A clear indication for labelling of GFP with the azobenzene-derivative 4-PAM is an absorbance increase at 320 nm (Figure 3A vs. 3B; see 4-PAM absorbance spectrum in Figure S1).

The procedure was repeated for the other three photostabilizers, although labelling could not be monitored by UV/VIS methods, because NPP, TX and COT show no characteristic absorbance at wavelengths  $> 300 \text{ nm}$ . Therefore, for these GFP-photostabilizer conjugates (GFP-COT, GFP-NPP, and GFP-TX), their spectroscopic characterization was performed using single-molecule TIRF (total internal reflection fluorescence) microscopy. The bulk emission spectra of unlabeled and all four labeled GFP-QC2 proteins were indistinguishable (Figure 2D)

supporting the idea that no static complexes between photostabilizer and chromophore were formed, e.g., complexes with blue-shifted absorption spectra.<sup>[27,48]</sup>

For single-molecule TIRF studies the proteins were immobilized on microscope coverslips according to published procedures<sup>[35]</sup> (for details see Material and Methods). Unlabeled GFP-QC2 fluorophores were observed as well-separated diffraction-limited fluorescence spots in camera images (Figure 4A). GFP-QC2 behaved similarly to other fluorescent proteins when studied on the single-molecule level featuring low photostability (Figure 4B), poor signal-to-noise ratio (SNR) and low brightness for both oxygenated and deoxygenated conditions (Figure 4C). Deoxygenated conditions can increase photon emission since oxygen may act as a fluorescence quencher or diminish photon emission if reactive-oxygen species mediate photobleaching pathways.<sup>[48,62,63]</sup> The analysis of detected GFP numbers in each movie frame (Figure 4B) and fluorescence time trace analysis (Figure 4C/5) using previously published procedures<sup>[35]</sup> allowed us to quantitatively determine the count-rate, SNR and photobleaching times for single molecules for different excitation intensities (0.4, 2.0, 3.2  $\text{kW}/\text{cm}^2$ ) in the absence and presence of oxygen (Figure 4D). For unlabeled GFP-QC2 fluorophores (Figure 4D), we observed short fluorescence periods of  $\sim 20 \text{ s}$  with count rates of  $\sim 0.5 \text{ kHz}$  at  $0.4 \text{ kW}/\text{cm}^2$  (see Figure 5 for individual traces). The SNR of GFP-QC2 at 100 ms binning was between 1.5–4 (Figure 4D).

The total number of detected photons were similar for most excitation conditions, i.e., between  $\sim 25000$ – $50000$ . The constant values resulted from faster photobleaching, but higher count-rate for increasing excitation intensity (Figure 4D). The normalized number of GFP-QC2 proteins per frame always showed an initial increase in the first 5–10 s that is consistent with previous reports of GFP/ $\alpha$ -GFP<sup>[56]</sup> and likely relates to photoconversion processes (Figure 4B). We thus analyzed photobleaching times *via* an exponential fit of the tail of the decay. We also studied the influence of known solution additives such as COT and TX as controls (Figure S2). These

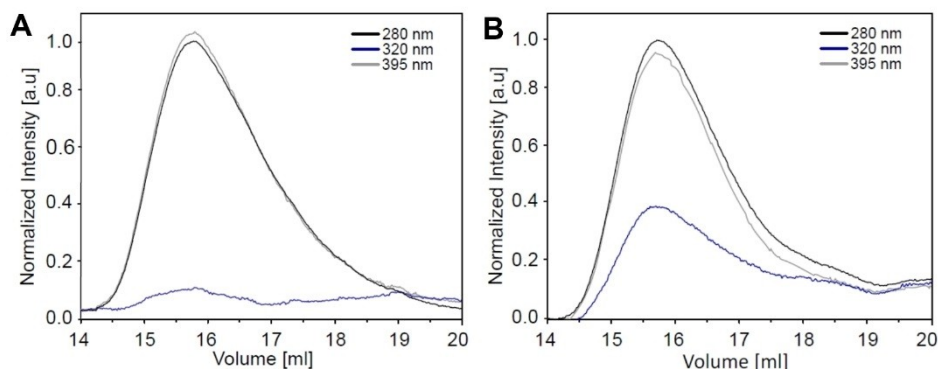


**Figure 3.** Size exclusion chromatograms of GFP-QC2 without (A) and with (B) 4-PAM showing an absorbance increase at 320 nm where PAM shows its maximum absorbance.



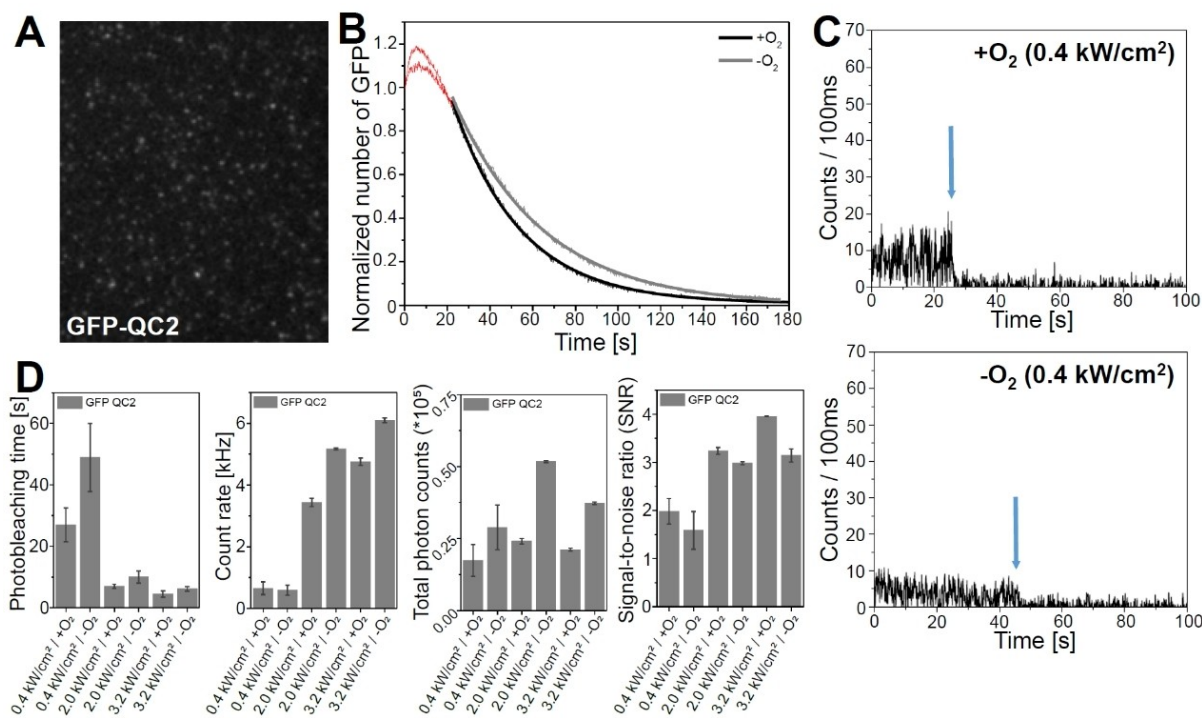


**Figure 4.** Quantitative photophysical characterization of GFP-QC2 in the presence and absence of oxygen under different excitation conditions following analysis methods described in Ref. [35]. (A) TIRF image with (B) bleaching analysis counting fluorophore number per frame as a function of time. (C) Fluorescent time traces of individual GFP-QC2 molecules (arrows indicate photobleaching) with (D) quantitative photophysical analysis under different excitation conditions. All experiments were repeated within independent biological repeats for at least three times. Bar graphs were derived from averages of > 5 movies per conditions per repeat.

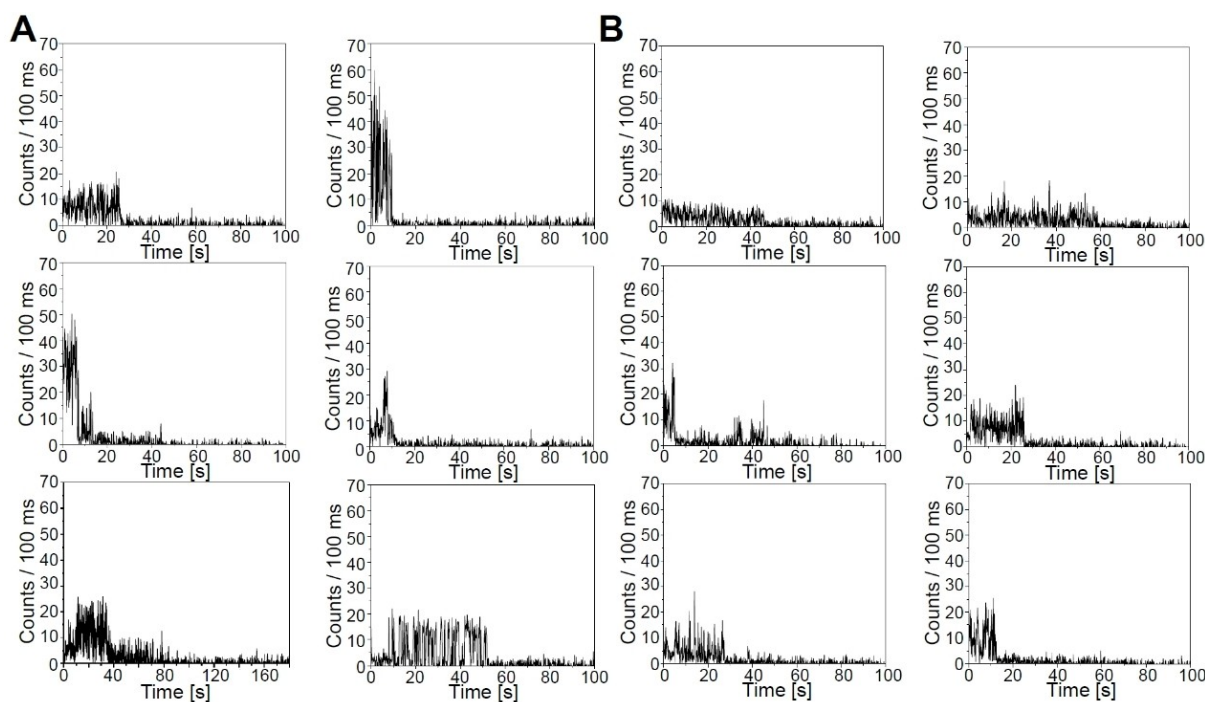


**Figure 5.** TIRF time traces of GFP-QC2 (A) in the presence and (B) in the absence of oxygen at  $0.4 \text{ kW/cm}^2$  excitation intensity.

experiments were done before we started our study on the intramolecular stabilizers to verify previous reports<sup>[52–54]</sup> that solution additives (and thus potentially also molecules attached outside the  $\beta$ -barrel) can influence the GFP-chromophore. For addition of both TX and COT, we found negative impacts on photobleaching rates, yet increased photon count-rates and constant total detected photons/SNR for single-immobilized GFP-QC2 molecules (Figure S2). Following these investigations, we tested covalent linkage of photostabilizers to the residues A206C and L221C (Figure 6).

The selected photophysical parameters were improved by conjugation of 4-PAM to GFP-QC2, referred to as GFP-AB (Figure 6). Photobleaching was retarded by 4-PAM for all conditions (Figure 6C), but most significantly in the absence of oxygen. Increases in the count-rate by AB were only observed in the absence of oxygen. SNR changes were found to be non-systematic. Strikingly, the increases of both count-rate and photobleaching time gave rise to a substantial gain in the total number of observed photons before photobleaching for all excitation conditions, especially in the absence of oxygen (Figure 6C).

As outlined before, the barrel of GFP-QC2 was also labeled with the photostabilizers TX, NPP, and COT to generate GFP-TX, GFP-NPA, GFP-COT, respectively (Figure 7); see SI for synthesis of photostabilizer maleimides and the labelling procedure.

These experiments revealed only minor effects of the different stabilizers on the photophysical behavior of GFP-QC2 in contrast to 4-PAM. None of these other photostabilizers increased or decreased the photobleaching time, count-rate, total photon count and SNR strongly. Trolox showed some exceptions of this general statement with elevated count-rates at 2 kW/cm<sup>2</sup>.

The observed small effects of TX, NPP, and COT were on one hand disappointing, albeit not surprising since other blue fluorophores (Cy2,<sup>[23]</sup> fluoresceins<sup>[37]</sup>) were shown to be only minimally affected by these stabilizers. Importantly, these data further support that the idea of a unique interaction between the FP-chromophore and 4-PAM, which was not seen with any other stabilizer.

### 3. Summary and Discussion

In this study, we showed that a mutant GFP with two specific cysteine (A206/L221C) residues available for labelling with commercial and custom-made maleimide-photostabilizers, exhibited increased photostability upon conjugation to the azobenzene derivative 4-PAM (abbreviated GFP-AB). It could, however, not be shown that the underlying mechanism for this improvement is related to triplet-state quenching. Triplet-state

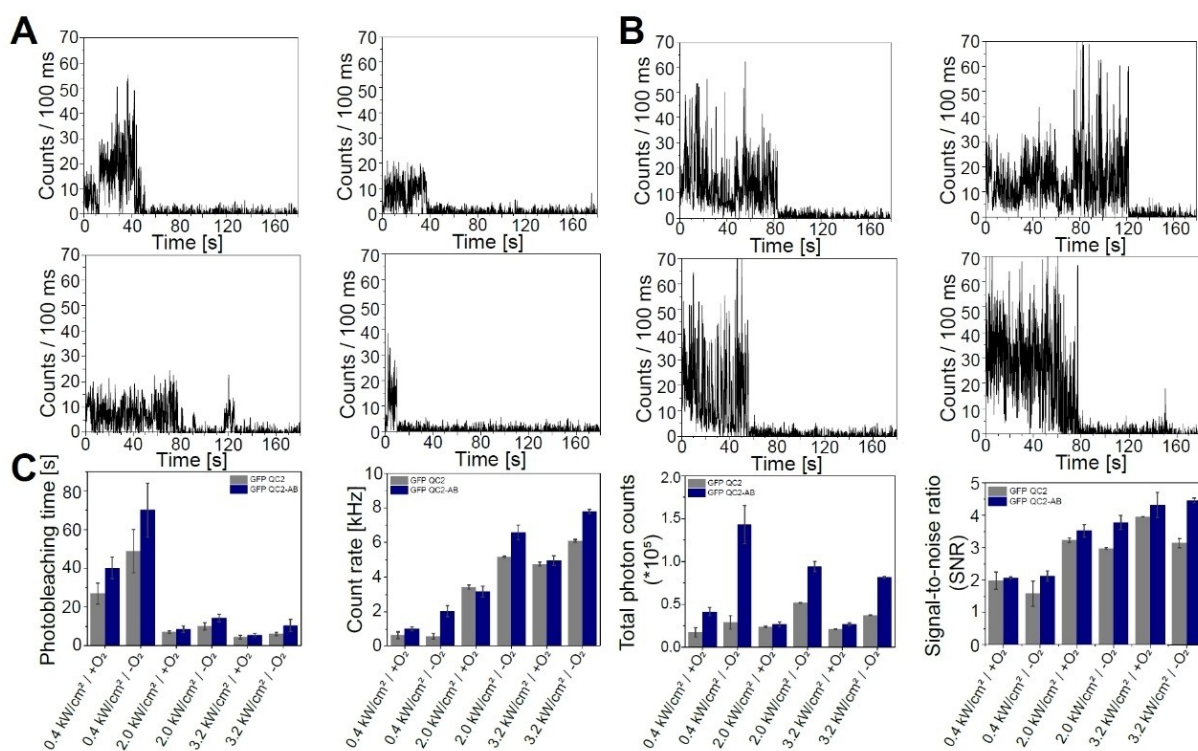


**Figure 6.** TIRF time traces of GFP-AB (A) in the presence and (B) in the absence of oxygen at 0.4 kW/cm<sup>2</sup> excitation intensity. (C) Quantitative photophysical analysis of GFP-AB under different excitation conditions.

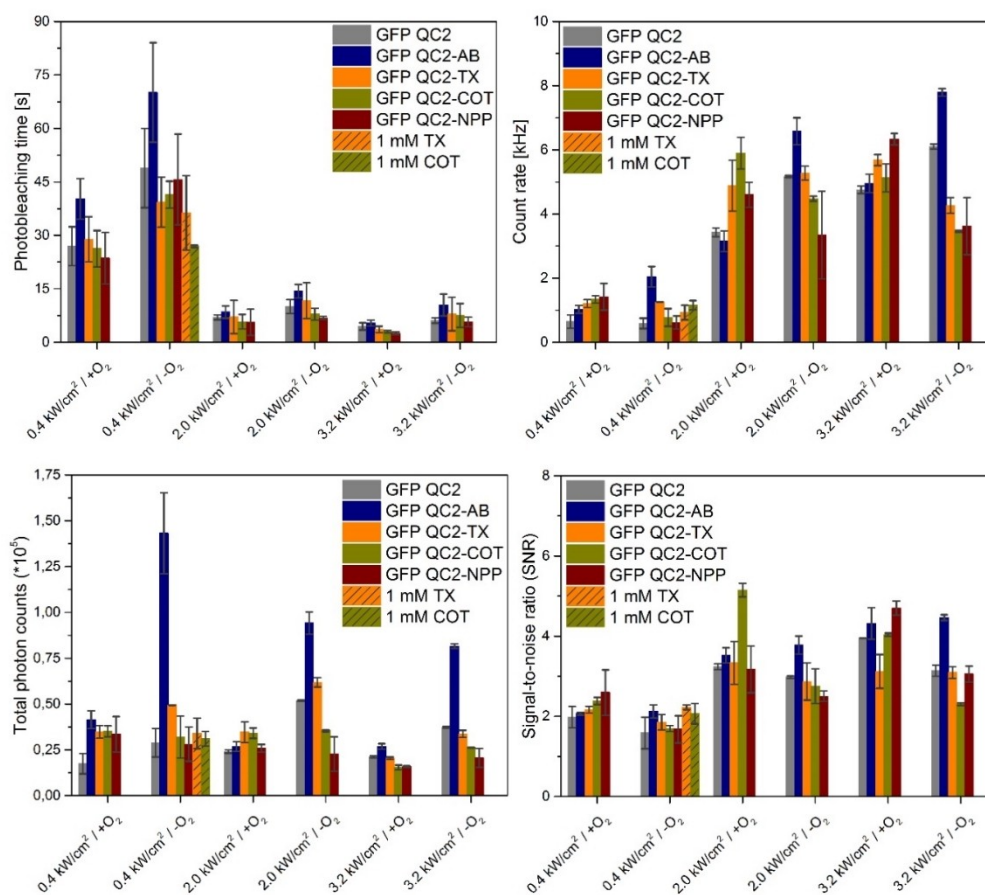


**Figure 7.** Quantitative photophysical characterization of GFP-QC2 with and without different photostabilizers in the presence and absence of oxygen at under different excitation conditions.

quenching was, however, demonstrated for the class of self-healing dyes,<sup>[25,26]</sup> which feature similar covalent linkage of photostabilizers to fluorophores.<sup>[29,64]</sup> The observed positive impact of 4-PAM on GFP photostability and the long recently determined triplet-state lifetimes of FPs,<sup>[40]</sup> however, supports the idea that FPs may be usefully targeted by intramolecular photostabilization, which provides an alternative approach to previous FP-improvement strategies using, e.g., chromophore fluorination.<sup>[65]</sup>

While our study paves the way for a systematic investigation of how to equip GFPs with suitable intramolecular photostabilizers, there are several issues that require further attention. The strategy to label GFP on the outside of the  $\beta$ -barrel may reduce efficient interaction between the chromophore and the photostabilizer. While there is convincing published evidence that the  $\beta$ -barrel does not shield the FP-chromophore fully<sup>[52–54]</sup> from interacting molecules in the buffer and also that triplet-quenching processes might be mediated by a contactless Förster mechanisms,<sup>[51]</sup> we speculate that selecting a residue inside the  $\beta$ -barrel might be even more promising for future studies. This could be done with residues such as C70 or other selected positions. In this case, a modified labelling strategy would be required, where the GFP is immobilized for labelling,

unfolded to make the internal residue accessible and refolded after labelling has occurred.

Ultimately, a major point of discussion is the type of photostabilizer and quenching mechanism (PET vs. energy transfer) required to successfully stabilize GFP. As for a number of blue-absorbing fluorophores (Cy2 or fluorescein), the common quenchers TX, NPP and COT were also ineffective for GFP. Fluorescein and other blue dyes have a triplet energy of 1.98 eV, which is much higher than those found for green- and red-emitting dyes with values between 1.46 eV (ATTO647N) and 1.72 eV (TMR).<sup>[37]</sup> The triplet-state of GFP was recently characterized and found to have a surprisingly low energy in the range of  $\sim 1.72$  eV.<sup>[40]</sup> This finding is not fully consistent with the fact that COT remains ineffective for GFP-QC2, since COT is very effective for ATTO647N. Generally, for blue fluorophores alternative quenchers with energetically higher-lying triplet-states such as azobenzene ( $\sim 2$  eV),<sup>[57]</sup> stilbene ( $\sim 2.4$  eV)<sup>[66]</sup> might be more optimal, also as solution additive for dyes with absorbance in the near-UV and blue spectral range. While these values for azobenzene's triplet state energy are higher in comparison to COT, azobenzene quenching was found to be effective for a range of different sensitizers with the highest triplet state energy in phenanthrene (triplet energy of 2.67 eV and  $k_q$  up to  $\sim 8.0 \times 10^9 \text{ M}^{-1} \text{ s}^{-1}$ ) and the lowest triplet state



energy in 3,4,8,9-dibenzopyrene (triplet energy of 1.49 eV and  $k_q$  up to  $\sim 1.0 \times 10^8 \text{ M}^{-1} \text{ s}^{-1}$ ).<sup>[57]</sup>

## Acknowledgments

This work was financed by an ERC Starting Grant (No. 638536 – SM-IMPORT to T.C.) and Deutsche Forschungsgemeinschaft (SFB863 project A13 & GRK2062 project C03 to T.C. and JU650/2-2 to G.J.). L. Zhang thanks the Alexander von Humboldt foundation for a postdoctoral research fellowship. J.H.M.vdV. acknowledges Ubbo-Emmius funding (University of Groningen). T.C. was further supported by Deutsche Forschungsgemeinschaft through the cluster of excellence CIPSM and by the Center of Nanoscience Munich (CeNS). We thank D. A. Griffith for sequencing of the GFP-QC2 plasmid, reading of the manuscript and thoughtful comments and suggestions. We thank J. H. Smit and S. Franz for support and discussions in the initial phase of the project. Open Access funding enabled and organized by Projekt DEAL.

## Conflict of Interest

The authors declare no conflict of interest.

**Keywords:** fluorescent proteins · spectroscopy · photophysics · photostabilization · self-healing dyes

- [1] M. Chalfie, Y. Tu, G. Euskirchen, W. W. Ward, D. C. Prasher, *Science* **1994**, *263*, 802–805.
- [2] R. Heim, D. C. Prasher, R. Y. Tsien, *Proc. Natl. Acad. Sci. USA* **1994**, *91*, 12501–12504.
- [3] G. S. Harms, L. Cognet, P. H. Lommerse, G. A. Blab, T. Schmidt, *Biophys. J.* **2001**, *80*, 2396–2408.
- [4] M. Ormö, A. B. Cubitt, K. Kallio, L. A. Gross, R. Y. Tsien, S. J. Remington, *Science* **1996**, *273*, 1392–1395.
- [5] O. Shimomura, F. H. Johnson, Y. Saiga, *J. Cell. Comp. Physiol.* **1962**, *59*, 223–239.
- [6] G. Crivat, J. W. Taraska, *Trends Biotechnol.* **2012**, *30*, 8–16.
- [7] P. J. Cranfill, B. R. Sell, M. A. Baird, J. R. Allen, Z. Lavagnino, H. M. De Gruiter, G.-J. Kremers, M. W. Davidson, A. Ustione, D. W. Piston, *Nat. Methods* **2016**, *13*, 557.
- [8] G. Jung, A. Zumbusch, *Microsc. Res. Tech.* **2006**, *69*, 175–185.
- [9] C. P. Toseland, *J. Chem. Biol.* **2013**, *6*, 85–95.
- [10] B. Ballou, B. C. Lagerholm, L. A. Ernst, M. P. Bruchez, A. S. Waggoner, *Bioconjugate Chem.* **2004**, *15*, 79–86.
- [11] M. Bruchez, M. Moronne, P. Gin, S. Weiss, A. P. Alivisatos, *Science* **1998**, *281*, 2013–2016.
- [12] C. P. Toseland, *J. Chem. Biol.* **2013**, *6*, 85–95.
- [13] G.-J. Kremers, S. G. Gilbert, P. J. Cranfill, M. W. Davidson, D. W. Piston, *J. Cell Sci.* **2011**, *124*, 157–160.
- [14] J. H. Bae, M. Rubini, G. Jung, G. Wiegand, M. H. Seifert, M. K. Azim, J.-S. Kim, A. Zumbusch, T. A. Holak, L. Moroder, *J. Mol. Biol.* **2003**, *328*, 1071–1081.
- [15] B. P. Cormack, R. H. Valdivia, S. Falkow, *Gene* **1996**, *173*, 33–38.
- [16] M. Zimmer, *Chem. Rev.* **2002**, *102*, 759–782.
- [17] B. T. Andrews, A. R. Schoenfish, M. Roy, G. Waldo, P. A. Jennings, *J. Mol. Biol.* **2007**, *373*, 476–490.
- [18] J.-D. Pédelacq, S. Cabantous, T. Tran, T. C. Terwilliger, G. S. Waldo, *Nat. Biotechnol.* **2006**, *24*, 79–88.
- [19] T. Brakemann, A. Stiel, *Nat. Biotechnol.* **2011**, *29*, 942–947.
- [20] N. C. Shaner, G. G. Lambert, A. Chamma, Y. Ni, P. J. Cranfill, M. A. Baird, B. R. Sell, J. R. Allen, R. N. Day, M. Israelsson, *Nat. Methods* **2013**, *10*, 407.
- [21] P. Dedecker, F. C. De Schryver, J. Hofkens, *J. Am. Chem. Soc.* **2013**, *135*, 2387–2402.
- [22] M. Kneen, J. Farinas, Y. Li, A. Verkman, *Biophys. J.* **1998**, *74*, 1591–1599.
- [23] R. B. Altman, Q. Zheng, Z. Zhou, D. S. Terry, J. D. Warren, S. C. Blanchard, *Nat. Methods* **2012**, *9*, 428–429.
- [24] J. H. van der Velde, E. Ploetz, M. Hiermaier, J. Oelerich, J. W. de Vries, G. Roelfes, T. Cordes, *ChemPhysChem* **2013**, *14*, 4084–4093.
- [25] B. Liphardt, B. Liphardt, W. Lüttke, *Opt. Commun.* **1981**, *38*, 207–210.
- [26] B. Liphardt, B. Liphardt, W. Lüttke, *Opt. Commun.* **1983**, *48*, 129–133.
- [27] J. H. Van Der Velde, J. Oelerich, J. Huang, J. H. Smit, A. A. Jazi, S. Galiani, K. Kolmakov, G. Gouridis, C. Eggeling, A. Herrmann, *Nat. Commun.* **2016**, *7*, 10144.
- [28] R. Dave, D. S. Terry, J. B. Munro, S. C. Blanchard, *Biophys. J.* **2009**, *96*, 2371–2381.
- [29] Q. Zheng, S. Jockusch, Z. Zhou, R. B. Altman, J. D. Warren, N. J. Turro, S. C. Blanchard, *J. Phys. Chem. Lett.* **2012**, *3*, 2200–2203.
- [30] Q. Zheng, M. F. Juetz, S. Jockusch, M. R. Wasserman, Z. Zhou, R. B. Altman, S. C. Blanchard, *Chem. Soc. Rev.* **2014**, *43*, 1044–1056.
- [31] Q. Zheng, S. Jockusch, Z. Zhou, R. B. Altman, H. Zhao, W. Asher, M. Holsley, S. Mathiasen, P. Geggier, J. A. Javitch, *Chem. Sci.* **2017**, *8*, 755–762.
- [32] V. Glembockyte, G. Cosa, *J. Am. Chem. Soc.* **2017**, *139*, 13227–13233.
- [33] P. Tinnefeld, T. Cordes, *Nat. Methods* **2012**, *9*, 426.
- [34] J. H. Smit, J. H. van der Velde, J. Huang, V. Trauschke, S. S. Henrikus, S. Chen, N. Eleftheriadis, E. M. Warszawik, A. Herrmann, T. Cordes, *Phys. Chem. Chem. Phys.* **2019**, *21*, 3721–3733.
- [35] J. H. van der Velde, J. Oelerich, J. Huang, J. H. Smit, M. Hiermaier, E. Ploetz, A. Herrmann, G. Roelfes, T. Cordes, *J. Phys. Chem. Lett.* **2014**, *5*, 3792–3798.
- [36] J. H. van der Velde, J. J. Uusitalo, L.-J. Ugen, E. M. Warszawik, A. Herrmann, S. J. Marrink, T. Cordes, *Faraday Discuss.* **2015**, *184*, 221–235.
- [37] Q. Zheng, S. Jockusch, G. G. Rodríguez-Calero, Z. Zhou, H. Zhao, R. B. Altman, H. D. Abruña, S. C. Blanchard, *Photochem. Photobiol. Sci.* **2016**, *15*, 196–203.
- [38] J. H. Van Der Velde, J. H. Smit, E. Hebisch, M. Punter, T. Cordes, *J. Phys. D* **2018**, *52*, 034001.
- [39] D. Sirbu, O. J. Woodford, A. C. Benniston, A. Harriman, *Photochem. Photobiol. Sci.* **2018**, *17*, 750–762.
- [40] M. Byrdin, C. Duan, D. Bourgeois, K. Brettel, *J. Am. Chem. Soc.* **2018**, *140*, 2897–2905.
- [41] F. Yang, L. G. Moss, G. N. Phillips, *Nat. Biotechnol.* **1996**, *14*, 1246–1251.
- [42] T. D. Craggs, *Chem. Soc. Rev.* **2009**, *38*, 2865–2875.
- [43] G. Cui, Z. Lan, W. Thiel, *J. Am. Chem. Soc.* **2012**, *134*, 1662–1672.
- [44] S. J. Remington, *Curr. Opin. Struct. Biol.* **2006**, *16*, 714–721.
- [45] A. Cramer, E. A. Whitehorn, E. Tate, W. P. Stemmer, *Nat. Biotechnol.* **1996**, *14*, 315–319.
- [46] H. Chen, S. S. Ahsan, M. E. B. Santiago-Berrios, H. D. Abruña, W. W. Webb, *J. Am. Chem. Soc.* **2010**, *132*, 7244–7245.
- [47] H. Chen, E. Rhoades, J. S. Butler, S. N. Loh, W. W. Webb, *Proc. Natl. Acad. Sci. USA* **2007**, *104*, 10459–10464.
- [48] J. R. Lakowicz, *Principles of Fluorescence Spectroscopy*, Springer, Heidelberg, **2013**.
- [49] A. C. Vaiana, H. Neuweiler, A. Schulz, J. Wolfrum, M. Sauer, J. C. Smith, *J. Am. Chem. Soc.* **2003**, *125*, 14564–14572.
- [50] A. Mamontova, A. Grigoryev, A. Tsarkova, K. Lukyanov, A. Bogdanov, *Russ. J. Bioorg. Chem.* **2017**, *43*, 625–633.
- [51] F. Schaefer, F.-G. Zhang, J. Jethwa, *Appl. Phys. B* **1982**, *28*, 37–41.
- [52] A. M. Bogdanov, E. I. Kudryavtseva, K. A. Lukyanov, *PLoS One* **2012**, *7*.
- [53] A. M. Bogdanov, A. S. Mishin, I. V. Yampolsky, V. V. Belousov, D. M. Chudakov, F. V. Subach, V. V. Verkhusha, S. Lukyanov, K. A. Lukyanov, *Nat. Chem. Biol.* **2009**, *5*, 459.
- [54] R. Saha, P. K. Verma, S. Rakshit, S. Saha, S. Mayor, S. K. Pal, *Sci. Rep.* **2013**, *3*, 1–7.
- [55] I. Jusuk, C. Vietz, M. Raab, T. Dammeyer, P. Tinnefeld, *Sci. Rep.* **2015**, *5*, 14075.
- [56] G. H. Patterson, S. M. Knobel, W. D. Sharif, S. R. Kain, D. W. Piston, *Biophys. J.* **1997**, *73*, 2782.
- [57] S. Monti, E. Gardini, P. Bortolus, E. Amouyal, *Chem. Phys. Lett.* **1981**, *77*, 115–119.
- [58] T. Cordes, D. Weinrich, S. Kempa, K. Riesselmann, S. Herre, C. Hoppmann, K. Rück-Braun, W. Zinth, *Chem. Phys. Lett.* **2006**, *428*, 167–173.
- [59] R. S. Ritterson, D. Hoersch, K. A. Barlow, T. Kortemme in *Design of Light-Controlled Protein Conformations and Functions*, Springer, Heidelberg, **2016**, pp. 197–211.



- [60] T. E. Schrader, W. J. Schreier, T. Cordes, F. O. Koller, G. Babitzki, R. Denschlag, C. Renner, M. Löweneck, S.-L. Dong, L. Moroder, *Proc. Natl. Acad. Sci. USA* **2007**, *104*, 15729–15734.
- [61] G. Gouridis, G. K. Schuurman-Wolters, E. Ploetz, F. Husada, R. Vietrov, M. De Boer, T. Cordes, B. Poolman, *Nat. Struct. Mol. Biol.* **2015**, *22*, 57.
- [62] C. E. Aitken, R. A. Marshall, J. D. Puglisi, *Biophys. J.* **2008**, *94*, 1826–1835.
- [63] R. E. Benesch, R. Benesch, *Science* **1953**, *118*, 447–448.
- [64] M. Isselstein, L. Zhang, V. Glembockyte, O. Brix, G. Cosa, P. Tinnefeld, T. Cordes, *J. Phys. Chem. Lett.* **2020**, *11*, 4462–4480.
- [65] S. Veettil, N. Budisa, G. Jung, *Biophys. Chem.* **2008**, *136*, 38–43.
- [66] J. Saltiel, D. Chang, E. Megarity, A. Rousseau, P. Shannon, B. Thomas, A. Uriarte, *Pure Appl. Chem.* **1975**, *41*, 559–579.

---

Manuscript received: June 9, 2021  
Revised manuscript received: July 2, 2021  
Version of record online: July 22, 2021